GEOPHYSICAL RESEARCH LETTERS, VOL. 28, NO. 17, PAGES 3259-3262, SEPTEMBER 1, 2001

The effect of CO_2 variability on the retrieval of atmospheric temperatures

Richard J. Engelen, Graeme L. Stephens, and A. Scott Denning

Department of Atmospheric Science, Colorado State University, Fort Collins, Colorado

Abstract. The effect of spatial variability of the atmospheric CO_2 distribution on temperature and water vapor retrievals from high spectral resolution observations of infrared emission is estimated by performing 4 different retrieval experiments. Using a global mean CO_2 value, as currently routinely used, introduces errors in the retrieved temperature profile of up to 0.85 K compared to a retrieval in which the CO_2 profile is known exactly. Including CO_2 in the retrieval vector reduces these errors to 0.3 K. A more practical alternative, especially for data assimilation, is to use a monthly mean zonal mean CO_2 value, which produces errors of up to 0.35 K in the temperature profile.

Introduction

Satellite retrievals of temperature profiles from observations of infrared emission are an important ingredient of the data assimilation process of numerical weather forecast (NWP) models. Although some NWP centers now directly assimilate radiances, the basic inversion problem remains the same. One of the assumptions in this retrieval process is that the atmospheric CO_2 concentration remains fixed and uniform and often is assigned outdated values. Recently, ECMWF adopted a global mean monthly mean vertically averaged CO_2 concentration (J.-J. Morcrette, personal communication, 2001), but this still does not reflect the extent of regional differences as shown in Figure 1. This figure shows the values used by ECMWF together with data from 4 different surface flask stations as compiled by GLOBALVIEW-CO2 [*GLOBALVIEW-CO_2*, 2000]. The aim of this paper is to estimate the errors in a temperature retrieval from high spectral resolution infrared data due to unaccounted regional variability of the CO_2 concentration.

Retrieval Theory

The retrieval experiments were performed using optimal estimation theory and are described in more detail in *Engelen et al.* [2001]. In such a retrieval strategy, the observations are weighted with an *a priori* constraint using the respective errors as weights. The observations in our retrieval simulations consist of the infrared spectrum between 500 cm^{-1} and 2500 cm^{-1} at 1 cm^{-1} spectral resolution analogous to the radiance data to be provided by the Atmospheric InfraRed Sounder (AIRS). The retrieved atmospheric variables are the temperature profile and the water vapor profile. The forward model that relates the atmospheric variables to the observations is a Malkmus radiative transfer model as described in *Engelen and Stephens* [1999] and *Engelen et al.* [2001]. It is a fast radiative transfer model based on the HITRAN96 data base [*Rothman*, 1998] and using the CKD2.4 continuum absorption [*Clough et al.*, 1989]. The measurement error of the radiances used to specify the measurement covariance matrix is 0.5%, which corresponds roughly to a 0.3 K error in brightness temperatures. The *a priori* profiles in our retrieval experiments are defined as random offsets by 0.8 K and 10 % specific humidity of the simulated "true" profiles. The *a priori* error estimates for temperature are taken to be 1 K and for water vapor 10 %, which is consistent with the background error standard deviation used in the ECMWF data assimilation [*Fillion and Mahfouf*, 2000]. Both the temperature and water vapor error covariances have off-diagonal elements representing correlations between the layers with a correlation length scale of 5 km. In the retrieval experiment where CO_2 is retrieved as well, the CO_2 profile is added to the retrieval vector as well as to the *a priori* vector. The *a priori* profile is defined as a zonal mean vertically mean CO_2 value with an uncertainty of 4 ppmv.

Simulated Data

Temperature, water vapor, and CO_2 concentration in the atmosphere and at the surface were simulated in the CSU General Circulation Model (GCM) [*Fowler and Randall*, 1999]. The model was integrated on a 4°x 5°latitude-longitude grid, with a 6-minute time step. The simulated CO_2 concentration was driven by prescribed exchange at the surface. These fluxes represent the sum of CO_2 emitted by fossil fuel combustion, air-sea gas exchange, and pho-

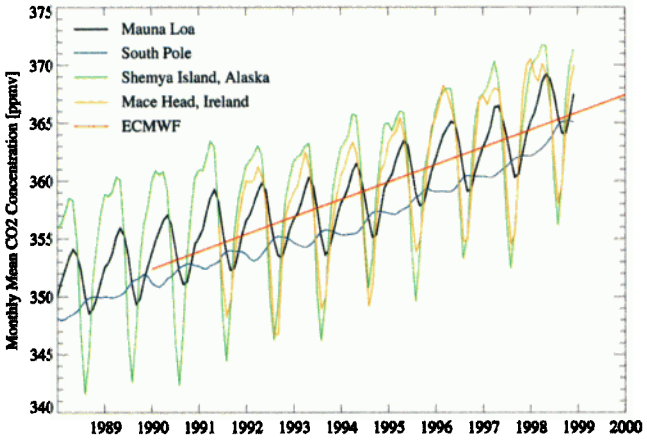

Figure 1. Time series of monthly mean surface CO_2 volume mixing ratios for 4 flask stations. The red line represents the values used by ECMWF.

Paper number 2001GL013496.
0094-8276/01/2001GL013496$05.00

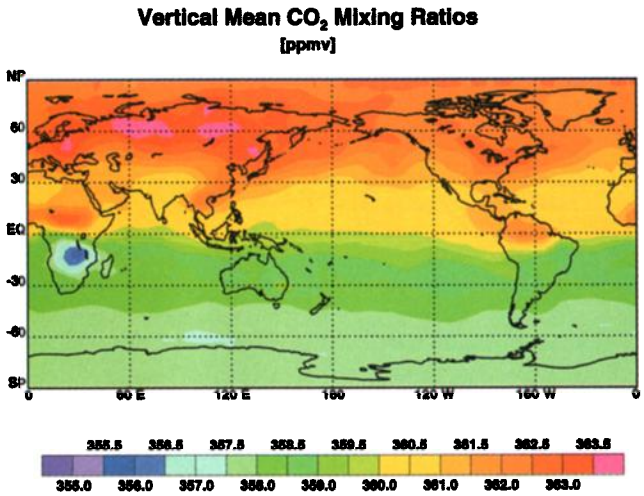

Figure 2. Column averaged CO_2 volume mixing ratio for a typical day in March.

tosynthesis and respiration at the vegetated land surface. Fossil fuel emissions (5.8 x 10^{12} kg C yr^{-1}, or Pg C yr^{-1}) were specified according to a-seasonal estimates from econometric data by *Andres et al.* [1996] and are believed to be accurate to within 10%. Air-sea gas exchange (with a globally integrated sink of 2.1 Pg C yr^{-1}) was specified according to estimates of *Takahashi et al* [2000], derived by interpolation of measured sea-surface pCO_2 data and a wind speed-dependent gas exchange coefficient. These fluxes are better constrained by data in the northern Atlantic than elsewhere, and are particularly uncertain in the Southern Ocean. The global integral is known to perhaps 30% [*Houghton et al.*, 1995]. Exchange with the terrestrial biosphere dominates the seasonal cycle of atmospheric CO_2, and produces very strong spatial gradients at any given time, yet has an annual magnitude smaller than the other flux components. We prescribed these exchanges according to the CASA model [*Randerson*, 1997], which uses satellite vegetation imagery and climate data to calculate photosynthesis, and a model of carbon turnover in vegetation and soils to specify respiration. To balance the globally averaged atmospheric carbon budget for a typical year requires a terrestrial sink in addition to the prescribed sources and sinks described above. The GCM was then used to calculate the resulting CO_2 concentration field due to the various surface exchange processes, advection, convection, and turbulent transport. The tracer transport characteristics of the CSU GCM have been shown to produce concentration fields that are in reasonable agreement with available observations [*Denning et al.*, 1996]. Simulated values were sampled hourly and interpolated to constant pressure surfaces, then averaged to produce daily mean fields. Boundary-layer values are calculated directly, since the PBL top is a coordinate surface in the CSU GCM [*Randall et al.*, 1992]. Results were analyzed for a day in March following a three year spin-up.

Results and Discussion

Figure 2 shows the simulated total column CO_2 distribution for March 1. The CO_2 distribution has a clear north-south gradient caused by both the rectifier effect [*Denning et al.*, 1999] of the terrestrial biosphere and the fossil fuel emissions. Over the northern continent CO_2 concentrations are the highest of the year, because photo-synthesis has not really started yet, while fossil fuel emission is large. The dipole-like structure over Africa is caused by the dependence of the balance between photosynthesis and respiration on the wet and dry seasons. For this particular day we performed 4 retrieval experiments: (i) a temperature and water vapor retrieval with exact knowledge of the CO_2 distribution, (ii) a temperature and water vapor retrieval with a prescribed global mean CO_2 concentration of 360 ppmv, (iii) a retrieval of temperature, water vapor and CO_2 combined, and (iv) a temperature and water vapor retrieval with a prescribed zonal mean CO_2 concentration. Figure 3a shows the root-mean-square (RMS) error over the retrieved temperature profile for each grid box between experiment (i) and (ii), where the RMS error is defined as:

$$\mathrm{RMS} = \sqrt{\frac{1}{N}\sum_{j=1}^{N}\left[T_{j,(i)} - T_{j,(ii)}\right]^2} \qquad (1)$$

where $T_{j,(i)}$ is the retrieved temperature at pressure level j for experiment (i), and N is the number of levels. The

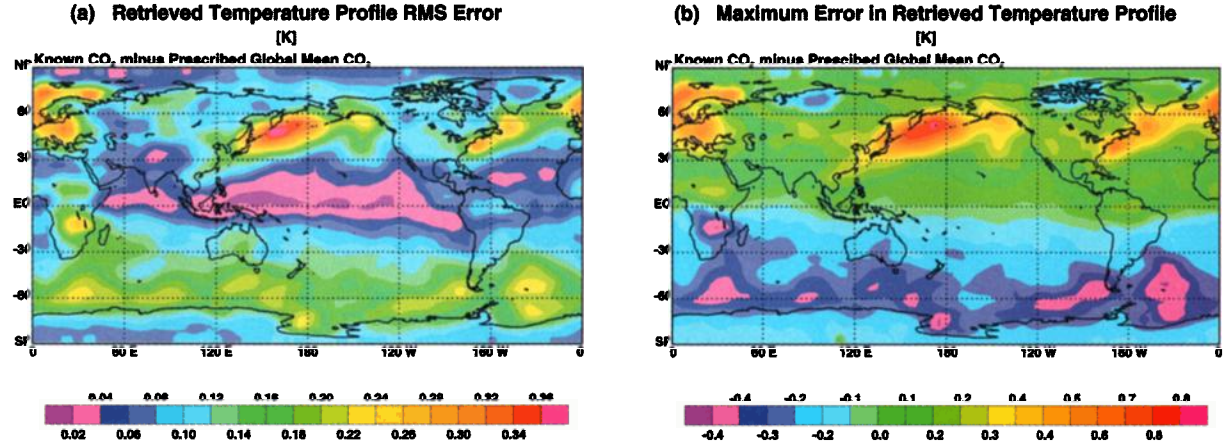

Figure 3. Root-mean-square error (a) and maximum error at any level (b) in every retrieved temperature profile when CO_2 is prescribed as a single monthly mean global mean value.

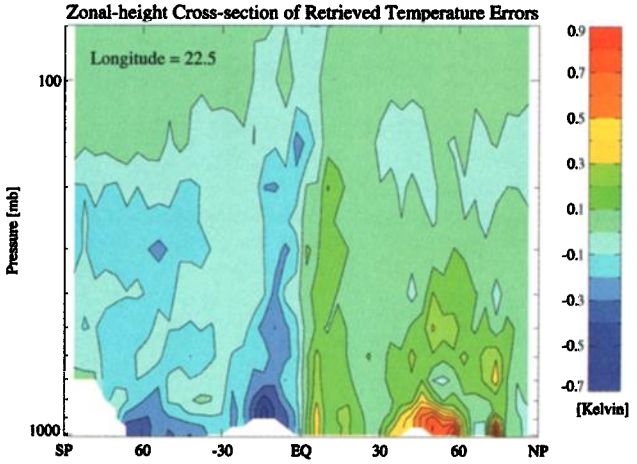

Figure 4. Zonal-height cross-section of the temperature retrieval errors when CO_2 is prescribed as a single monthly mean global mean value.

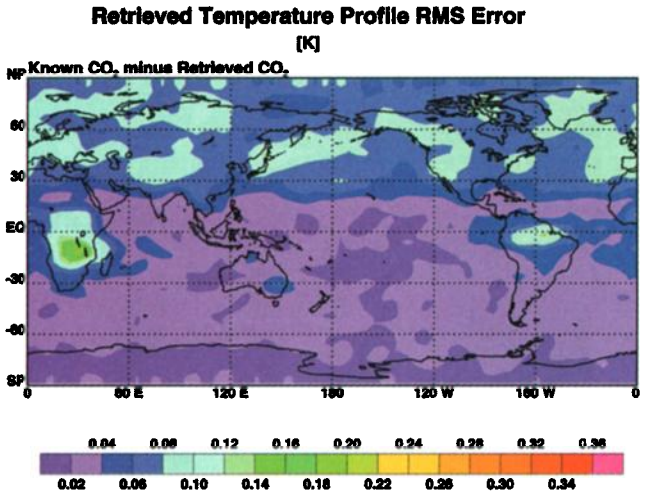

Figure 6. Same as Figure 3a, but with CO_2 prescribed as a monthly mean zonal mean value.

maximum error in the retrieved temperature profile for each grid box is shown in Figure 3b. This maximum error can in principal occur at any pressure level and is a measure of the amplitude of the errors. Both figures show significant errors in the temperature retrieval that are caused by using a single global mean CO_2 value instead of the actual concentration profiles. RMS errors up to 0.35 K are made in the northern hemisphere with individual level errors up to 0.85 K. Largest errors are located in the downwind plumes from industrialized areas, where CO_2 concentrations are elevated in the lower troposphere. The relatively low errors over the northern continents are due to the low water vapor content in those areas, which makes the temperature retrieval less affected by the uncertainty in the retrieved water vapor profile and therefore less dependent on the uncertainties in the CO_2 values. Higher errors are also found over the southern ocean, where the CO_2 values in the lower troposphere are significantly lower than the global mean value of 360 ppmv. CO_2 profiles over the tropical oceans are generally well mixed (due to the large convection) and close to the global mean value of 360 ppmv. Therefore these areas have very small errors in the temperature profiles. Figure 4 shows a zonal-height cross-section at 22.5° longitude (Eastern Europe, Africa) of the temperature retrieval errors for this experiment. Retrieval errors over Europe (50° north) are mainly contained in the lower troposhere, while retrieval errors over Africa are also significant in the mid- and upper troposphere due to the large convection that transports the CO_2 anomalies, and thus the temperature retrieval errors, to higher altitudes.

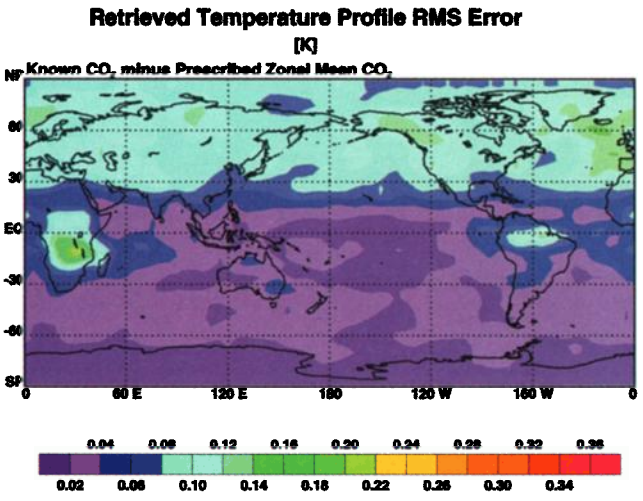

Figure 5. Same as Figure 3a, but with CO_2 included as a variable in the retrieval.

Figure 5 shows the RMS differences between experiment (i) and (iii). The figure shows that the errors in the temperature retrieval are significantly reduced by retrieving CO_2 as well instead of prescribing CO_2 with a single global mean value. Although the retrieval of CO_2 in the infrared is not perfect and is weighted to the mid- and upper troposphere [*Engelen et al.*, 2001], the impact on the temperature retrieval is clear. The differences that remain are due to the imperfect retrieval of CO_2 in the lower troposphere.

The last experiment (iv) uses a prescribed monthly mean zonal mean CO_2 distribution in the temperature and water vapor profile retrieval. A zonal mean CO_2 distribution is available from the current surface flask network and better reflects the seasonality. Figure 6 shows the RMS differences between this experiment and experiment (i). Although the errors are slightly larger than in the experiment with the included CO_2 retrieval, errors are significantly reduced from the experiment with a single global mean value. This result is important, since it is much more practical to use a prescribed zonal mean than to perform a full CO_2 retrieval or assimilation.

The results presented above are dependent on the choice of the covariance matrices, that define the weighting between the observations and the *a priori* constraint in the estimation approach [*Rodgers*, 2000]. These matrices also define the covariance matrix of the retrieved atmospheric variables. If the variance in the *a priori* covariance matrix is increased (more uncertainty in the *a priori* values), the retrieved temperature profile will be defined more by the observations. This amplifies the sensitivity on the errors in the CO_2 concentrations. On the other hand, if the variance

in the measurement covariance matrix is increased (more measurement noise), the retrieved profiles are more defined by the *a priori* constraint and therefore less dependent on the errors in the CO_2 concentrations. As already noted for the northern continents, the dependence of the temperature retrieval on the CO_2 values is also a function of the water vapor content. In the dry continental winter, this reduces the sensitivity on the CO_2 values as shown above, while in the moister continental summer errors over land (where the CO_2 deviations from the global mean are the largest) become larger than the errors over the ocean (not shown).

Conclusions

Four retrieval experiments were performed to estimate the effect of regional variations in the CO_2 concentration on a temperature retrieval from high spectral resolution infrared data. The base retrieval retrieved temperature and water vapor profiles for a day in March with CO_2 profiles exactly known. The three other retrieval experiments used a prescribed global mean value of 360 ppmv, retrieved CO_2 profiles together with the temperature and water vapor profiles, and used a prescribed zonal mean CO_2 distribution, respectively. With the specified measurement uncertainty and uncertainty in the *a priori* constraint, maximum errors up to 0.85 K are made in the experiment with prescribed CO_2. The profile RMS error has values up to 0.35 K. Retrieving CO_2 together with temperature and water vapor brought the maximum errors down to 0.3 K and the profile RMS error down to 0.16 K. A good alternative for including the CO_2 retrieval is to prescribe a monthly mean zonal mean CO_2 value. Errors are almost as small as with the included CO_2 retrieval. Although all the above errors depend on the specification of the used covariance matrices, they are significant enough to have an effect on temperature retrievals or data assimilation.

Acknowledgments. The work described in this paper was supported by DOC-NOAA Contract NA67RJ0152 Amend 25 and NASA subcontract SA2805-23941.

References

Andres, R., G. Marland, I. Fung, and E. Matthews, A 1 x 1 distribution of carbon dioxide emissions from fossil fuel consumption and cement manufacture, 1950-1990, *Global Biochemical Cycles*, *10*, 419–430, 1996.

Clough, S., F. Kneizys, and R. Davis, Line shape and the water vapor continuum, *Atmospheric Research*, *23*, 229–241, 1989.

Denning, A.S., D. Randall, G. Collatz, and P. Sellers, Simulations of terrestrial carbon metabolism and atmospheric CO_2 in a general circulation model. Part 2: Spatial and temporal variations of atmospheric CO_2, *Tellus*, *48B*, 543–567, 1996.

Denning, A., T. Takahashi, and P. Friedlingstein, Can a strong atmospheric CO_2 rectifier effect be reconciled with a "reasonable" carbon budget, *Tellus*, *51B*, 249–253, 1999.

Engelen, R. J., and G. L. Stephens, Characterization of water vapour retrievals from infrared TOVS radiances and microwave SSM/T-2 radiances., *Q. J. R. Meteorol. Soc.*, 1999.

Engelen, R. J., A. S. Denning, K. R. Guerney, and G. L. Stephens, Global observations of the carbon budget: I. Expected satellite capabilities in the EOS and NPOESS eras., *J. Geophys. Res., in press*, 2001.

Fillion, L., and J.-F. Mahfouf, Coupling of moist-convective and stratiform precipitation processes for variational data assimilation, *Mon. Wea. Rev.*, *128*, 109–124, 2000.

Fowler, L., and D. Randall, Simulation of upper-tropospheric clouds with the CSU general circulation model, *J. Geophys. Res.*, *104*, 6101–6121, 1999.

GLOBALVIEW-CO_2, Cooperative Atmospheric Data Integration Project - Carbon Dioxide. CD-ROM, NOAA CMDL, Boulder, Colorado [Also available on Internet via anonymous FTP to ftp.cmdl.noaa.gov, Path: ccg/co2/GLOBALVIEW], 2000.

Houghton, J., L. Filho, B. Callandar, N. Harris, A. Kattenberg, and K. Maskell, *Climate Change 1995: Contribution of Working Group 1 to the Second Assessment Report of the Intergovernmental Panel on Climate Change*, Cambridge University Press, New York, 1995.

Randall, D., et al., A revised land-surface parameterization (SiB2) for atmospheric GCMs. Part 3: the greening of the CSU general circulation model, *J. Atm. Sci.*, *49*, 1903–1923, 1992.

Randerson, J., The contribution of terrestrial sources and sinks to trends in the seasonal cycle of atmospheric carbon dioxide, *Global Biogeochemical Cycles*, *11*, 535–560, 1997.

Rodgers, C. D., *Inverse methods for atmospheric sounding. Theory and practice.*, World Scientific, 2000.

Rothman, L., et al., The HITRAN molecular spectroscopic database and HAWKS (HITRAN Atmospheric Workstation): 1996 edition, *J. Quant. Spectrosc. Raiat. Transfer*, *60*, 665–710, 1998.

Takahashi, T., R. Wanninkhof, R. Feely, R. Weiss, D. C. N. Bates, J. Olafsson, C. Sabine, and S. Sutherland, Net sea-air CO_2 flux over the global oceans: An improved estimate based on the sea-air pCO_2 difference, in *Proceedings of the 2nd CO_2 in Oceans Symposium, Tsukuba, JAPAN, January 18-23, 1999*, vol. in press, 2000.

R. J. Engelen, G. L. Stephens, and A. S. Denning, Department of Atmospheric Science, Colorado State University, Fort Collins, CO 80523. (e-mail: richard@atmos.colostate.edu)

(Received May 24, 2001; revised June 21, 2001;
accepted June 26, 2001.)